INTERFACE ADHESION OF E-GLASS FIBERS IN MODEL POLYISOCYANURATE NETWORKS

W. G. McDonough, G. A. Holmes, and R. C. Peterson
National Institute of Standards and Technology
Polymers Division
Gaithersburg, Maryland 20899

ABSTRACT

Recent work examining the nature of the failure process of glass/epoxy specimens in the single fiber fragmentation test showed that the matrix exhibited pronounced non-linear viscoelastic behavior during the test, and that the interfacial shear strength value obtained was dependent on the rate of testing. Furthermore, it was demonstrated that the load in the sample at the end of the test was much lower than the value predicted by assuming linear-elastic behavior, and that the first fragment break occurred when the actual load in the matrix deviated from the linear-elastic prediction. To study these issues further, the testing protocol was repeated using a polyisocyanurate resin to see if a similar nonlinear viscoelastic response was observed. One result from this recent study was that the polyisocyanurate matrix did show nonlinear viscoelastic behavior similar to the epoxy matrix. Interestingly, from preliminary results, the fiber fragmentation distribution of the glass/polyisocyanurate specimens was found to be independent of the strain rate used during the test, so that the calculated interfacial shear strength appears rate independent. This result contrasted with that of the glass/epoxy specimens where the fiber fragmentation distribution, and thus, the measured interfacial shear strength, was dependent on the rate of strain.

INTRODUCTION

Urethane based composites made by the structural reaction injection molding (SRIM) process have been used by the Automotive Composites Consortium (ACC) in automotive applications. As with most composites, adhesion between the fiber and matrix is critical for the performance and long term durability of a composite part. Interface adhesion and durability studies often utilize the single fiber fragmentation test (SFFT) to assess these parameters (1). Central to the generation of reliable and useful data from this test is the preparation of network structures in the test samples comparable to those made in the composite part. Hence, several approaches have been used to make SRIM SFFT specimens. The SRIM process involves impingement mixing of the polyol, isocyanate, and catalyst, and injecting the mixture into a heated mold cavity previously packed with reinforcement. The cycle time is usually a few minutes. The problem with trying to make single fiber composites from the isocyanurate system used in the SRIM process described above is that SRIM entails very fast processing at high injection pressures. This process is impractical for single fiber composites because the fibers would not survive the injection pressures. Making specimens using SRIM has proven to be

difficult and no reliable procedure has been developed. The problem with polyisocyanurates, as well as polyurethanes, is that they foam very rapidly at room temperature and atmospheric pressure. Further, the catalyst plays an important role in setting the speed of the foaming process, and if one were to reduce the level of the catalyst, one should be able to extend the gel time, thus resulting in longer times to process the samples. However, even solving the problem of processing time would still leave the problem of the bubbles caused by the reaction with water. Previous research has shown that, with the addition of pressure using an inert gas, N_2, it is possible to suppress the formation of bubbles in making fragmentation specimens (2). Reproducible specimens using a reduced catalyst level have been prepared by an autoclave procedure. Since the catalyst, 1,4-diazabicyclo(2,2,2) octane, acts as a "true" catalyst in the crosslinking reaction, it is possible that comparable networks can be prepared using the autoclave procedure by applying appropriate postcuring procedures

In the single fiber fragmentation test, a dogbone is made with a resin having a high extension to failure and a single fiber embedded down the axis of the dogbone. The sample is pulled in tension and stress is transmitted into the fiber through the fiber-matrix interface (3). Since the fiber has a lower strain to failure than the resin, the fiber breaks as the strain is increased. This process continues until the remaining fiber fragments are all less than a critical transfer length. The critical transfer length is the length below which the fragments are too short for sufficient load to be transmitted into them to cause failure, and this point is termed saturation. The fragment lengths at saturation are measured and a micro-mechanics model is used to convert the average fragment length into a measure of the interface strength or stress transfer efficiency. The equation used is as follows:

$$\tau_{f_{max}}\{l_c\{t,M\},t\} = \frac{d\beta\{\varepsilon,t\}}{4} \frac{\sinh\beta\{\varepsilon,t\}(l_c\{t\}/2)}{\cosh\beta\{\varepsilon,t\}(l_c\{t\}/2)-1} \sigma_f\{l_c\{t\}\}$$

where

$$\beta\{\varepsilon,t\} = \frac{2}{d}\left[\frac{E_m\{\varepsilon,t\}}{(1+v_m)(E_f - E_m\{\varepsilon,t\})\ln(2r_m/d)}\right]^{1/2}$$

τ_{fm} denotes the interfacial shear strength
σ_f denotes the strength of the fiber at the critical length
E_f denotes the secant modulus of the fiber
E_m denotes the matrix modulus
v_m denotes the Poisson's ratio of the matrix
r_m denotes the radius of the matrix
D denotes the diameter of the fiber
l_c denotes the critical length of the fiber at saturation

During the SFFT, the specimens are strained incrementally and, after each strain increment, there is usually a pause before the next step-strain. Observations and experiments conducted in this laboratory have shown that the fiber fragmentation process is time-dependent to some degree (4). A 10 min pause between step-strains has been found to give reproducible

results. To investigate the rate dependency of the fiber fragmentation process further, three different pause times were used in this experiment.

Fragmentation of E-glass fibers during interfacial adhesion tests of an epoxy SFFT specimen have been shown by Holmes et al. to occur when the matrix is exhibiting nonlinear viscoelastic behavior (5). Previous work showed that the autoclaved polyisocyanurate SFFT specimens exhibited a higher extensibility than the diglycidyl ether of Bisphenol A/m-phenylene diamine (DGEBA/m-PDA)/E-glass test specimens, therefore, it is plausible that this matrix also exhibits nonlinear viscoelastic behavior during fiber fragmentation. Hence, a nonlinear analysis procedure is required to assess the interfacial shear strength at the fiber matrix interface. One conclusion of the research by Holmes was that linear-elastic and linear-viscoelastic predictions do not provide reasonable estimates of the actual load-time curve. Work has been progressing on modeling the fragmentation process in light of this nonlinear viscoelastic behavior. This research was presented at a recent workshop held at NIST on Micro-Mechanics Measurement Technologies for Fiber-Polymer Interfaces (6) and is addressing one of the three major needs identified at the workshop, namely, to improve the failure analysis with realistic materials and failure models.

EXPERIMENTAL STUDIES (7)

MATERIALS

Single filaments (unsized E-glass made by Owens-Corning) were separated from a fiber bundle with care being taken to touch only the ends of the fiber. The two-part resin system consisted of isocyanate (Spectrim ® MM 364-A from the Dow Chemical Company) and polyol (Spectrim ® MM 364-B from the Dow Chemical Company. The catalyst used was (1,4-diazabicyclo(2,2,2) octane (Dabco 33-LV from Air Products and Chemicals, Inc. Both the polyol and isocyanate were kept over phosphorus pentoxide in a desiccator for at least four weeks before processing to minimize moisture that may affect the processing.

PROCESSING

Sample preparation

The first step in making single fiber fragmentation samples was to make an eight-cavity mold out of RTV-664 from General Electric following the procedure described by Drzal et al. (3). All molds were post-cured at 150 °C and rinsed with acetone prior to use. Single filaments were separated from a fiber bundle with care being taken to touch only the ends of the fiber. Each cavity in the mold has sprue slots in the center of each end to aid in aligning the fiber in the center of the cavity. Once the fibers were in the cavities, they were fixed in place by putting a small drop of five-minute epoxy (Hardman Adhesives) at the far end of each sprue slot. Once the epoxy had hardened, the resin was ready to be prepared.

Although many attempts were made to make single fiber test samples, the simplest procedure was to keep the mass ratio of isocyanate to polyol at the same level as in the SRIM process: 2.4/1. However, the catalyst level was reduced from 0.015 mass fraction of polyol to 0.004 mass fraction of polyol. First, the catalyst was added to the polyol and stirred the liquid

for 30 s, then we added the isocyanate to the mixture and stirred for 30 s. Subsequently, the resin was poured into the mold cavities and transferred the mold to an autoclave (Minibond from United McGill Corporation).

The cure cycle called for pressurizing the chamber to 0.34 MPa above atmospheric pressure, while holding the temperature to 24 °C. Once the pressure inside the autoclave reached 0.34 MPa, the temperature and pressure were raised simultaneously. The temperature was raised at 2.5 °C/minute to 93 °C as the pressure was increased to 0.55 MPa above atmospheric pressure. The mold was held at 93 °C and 0.55 MPa for 30 minutes, then the pressure was reduced quickly to atmospheric pressure and the temperature was quickly cooled to 66 °C, and then the mold was cooled slowly overnight to room temperature. Subsequently, the samples were post-cured in an oven (Blue M model number MP-256C-1) for 1 h at 150 °C and then slow cooled to room temperature. Finally, the samples were removed from the mold and examined under the microscope. Valid samples were regarded as those that had no air bubbles, and whose fibers remained straight.

TESTING

Specimens were prepared for testing by sanding their ends and sides. The sanding had the dual effect of permitting the samples to fit in the grips of the testing apparatus and removing any surface microcracks that could have led to premature failure of the specimen. After the samples had been sanded, two marks were placed on the specimen surface around 1 cm apart and perpendicular to the axis of the specimen. These marks were used subsequently to measure the strain in the specimen during the test. After this preparation, the dimensions of the specimen (width and thickness) were measured.

The single fiber fragmentation tests were carried out on a small, hand operated testing apparatus such as that described by Drzal (3). This apparatus was attached to a Nikon Optiphot-Pol polarizing microscope. The stationary grip of this apparatus was attached through a load jig through a 1.1 kN load cell (Cooper Instruments, LPM 530), the details of which are given in Hunston, et al.(8). With the sample in the apparatus, fiber diameters were measured at 19 different locations along the fiber. During the test, a small step strain was applied manually by turning a knob attached to the movable grip of the apparatus. After each strain increment, there is usually a pause before the next step-strain. For this work, three different strain histories were used. For the first history, after each strain increment, a 10 min pause was observed consistently through the test. At each increment, the number of fragments and the strain were recorded. At saturation, the fragment lengths were also measured. The microscope had a video camera (Optronics LX-450A RGB Remote-Head microscope camera) and an optical micrometer (VIA-100 from Boeckeler) attached to it, allowing us to measure the fiber diameters and the fragment lengths. Fragment lengths were measured with the aid of a transducer (Trans-Tek, Inc. model 1002-0012). For the second strain history, a 10 min pause was initially observed between each strain increment. This time, however, instead of just recording the number of breaks, the fragment lengths were also measured. Once the number of fragments exceeded a certain number, it became physically impossible to complete all of the measurements in under 10 min, and more time was needed between increments until saturation was reached. This history was designated the 10 min variable test. Finally, the third history involved pause on 1 h at each strain increment. During this pause, fragment lengths were measured, and all fragment length measurements could be made, resulting in constant loading history. After each type of test was completed, the specimens were unloaded and allowed to relax to zero stress, and the fragment

lengths were again measured. The zero stress data was used to calculate the interfacial shear strength values.

The standard uncertainty in the instrument in measuring a point along the fiber is 0.3 μm. The standard uncertainty in relocating a point along the fiber reproducibly is 1.3 μm. The expected relative standard uncertainty of the load measurement is 3 %. The standard uncertainty in the measurement of the specimen dimensions and the radius of the matrix was 0.005 mm. The standard uncertainty of the measurement of the fiber diameter was 0.3 μm. The expected relative standard uncertainty in the stress measurement of the sample is 6 %. The expected relative standard uncertainty in the strain measurement is 3 % of the measured value. The expected relative standard uncertainty of the fiber strength at the critical length is 3 % of the measured value, and the expected combined relative standard uncertainty of β and τ is 6 %. The value of the fiber modulus was taken from Schultheisz et al. (10), and the value for the Poisson's ratio for the matrix was taken from Whitney et al. (11). The average application time of each strain step was 1.10 s and the average deformation was 14.4 μm , with the standard uncertainties for these measurements 0.2 s and 3.0 μm respectively. The strain was found to increase by 3.4×10^{-5} for each 1 N change in load during the relaxation of the specimen between strain steps because of compliance in the load frame. The standard deviation is within one standard deviation.

RESULTS AND DISCUSSION

In Figure 1, the load-time profile of a polyisocyanurate SFFT specimen is shown (lower curve). This specimen was strained at 10 min time intervals between each step-strain. Consistent with results obtained on DGEBA/m-PDA SFFT specimens (9) (Figure 2), the polyisocyanurate network exhibits pronounced viscoelastic behavior during the test. Using the small strain modulus, the linear elastic load time curve is shown for comparison. Although excellent agreement is obtained for the initial strain increments, the actual load in the end of the test is approximately 45 % lower than the value predicted by the linear elastic load time curve. In addition, the first fragment break appears when the actual load in the matrix has deviated from the linear elastic prediction. Previous calculations on DGEBA/m-PDA SFFT specimens have shown that the linear viscoelastic prediction does not provide a reasonable estimate of the actual load-time curve. As with the DGEBA/m-PDA SFFT specimens, the relaxation behavior of the matrix, within each step, becomes more pronounced as the strain is increased. This behavior is consistent with nonlinear viscoelastic behavior.

"Pseudo-isochronal" stress versus strain plots from the data given in Figure 1 are shown in Figure 3. By this term, it means that the clock will be figuratively restarted after each loading step so that comparisons can be made of the loads after each loading step at the same time into that step. For example, the 10 min data is the load recorded 10 min after each loading step was applied, i.e., the previous peak load. Figure 3 shows data at 10 s (10 s stress) and 10 min (10 min stress) for the sample shown in Figure 1. Linear regression analyses of the small strain and large strain 10 s stress data are also shown in Figure 3. The small strain modulus is 2.72 GPa, while the localized tangent modulus at large strains is 0.59 GPa. Also shown in Figure 3 is the location of the strain at which the first fiber break occurs, 0.0145.

In Figure 4, 10 s stress-strain plots of polyisocyanurate SFFT specimens tested at different loading rates are shown. In addition to the 10 s stress–strain plot for the specimen strained at 10 min intervals between step strains, specimens strained at variable times between step-strains and 1 h between step-strains are shown. For all specimens, the stress-strain

behavior of the polyisocyanurate networks at small strains are similar. For strains after the onset of yield, the 10 min and 1 h between step-strain specimens exhibit parallel curves, with the 1 h between step-strain specimen having a lower stress than the 10 min specimen at comparable strain values. This behavior is consistent with additional relaxation of the matrix stress with the increased time between step-strains. Since the specimen strained at variable times between strain increments was initially strained before the occurrence of any breaks at an interval of 10 min between step-strains, the stress strain behavior of this curve initially approximates that of the 10 min between strain increment stress-strain curve. As the number of breaks increased and the time between strain increments increased with the time required to measure the breaks, the stress strain behavior of the variable time between step-strain curve parallels that of the 1 h between step-strain curve at higher strains. For the three SFFT specimens shown in Figure 4, the first fiber break failure strains are consistent with data obtained from DGEBA/m-PDA SFFT test specimens (9).

The fragment distributions at saturation of the three SFFT specimens shown in Figure 4 are shown in Figure 5. The distributions and number of breaks at comparable sampling lengths are similar, even though the total time of the test was extended from 6 h to 36 h (see Figure 6). The means and standard deviations of the fragment distributions are given in Table I. The single factor analysis of variance was run and showed that the results from the three samples were equivalent (P = 0.35). These initial results indicate that strain rate does not affect the fragment distribution at saturation. This conclusion contrasts with the conclusion obtained on DGEBA/m-PDA SFFT specimens. In the DGEBA/m-PDA network, a significant change in the fragment distribution was observed when the strain rate was increased from 16 h to 30 h (P = 0.0003).

To calculate the interfacial shear strength from this experimental data, the strength of the fiber at the critical transfer length must be determined. This value was estimated by plotting the log of the number of breaks with increasing strain for each polyisocyanurate SFFT specimen (see Figure 7). For specimens 1 and 2, there is a clear break in the rate of fragment production at approximately 0.03 strain. Taking the modulus of the E-glass fiber to be 67.5 GPa, the strength of the fiber at critical length for these two specimens was estimated to be 2.0 GPa. The rate of fragment production in the third specimen changes at approximately 0.024 strain. However, this initial change does not coincide with the final rate of fragment production at strain values greater than 0.03 strain. The three measurements (delineated by the solid triangle in the figure) between 0.024 and 0.030 strain were averaged and a value of 1.8 GPa was taken as an alternative to using the 2.0 GPa value. Calculations for specimen 3 using both values, with the corresponding secant modulus, are shown in Table I. The interfacial shear strength obtained by using the secant modulus is approximately 13 % lower than the value obtained using an elastic modulus value of 3.06 GPa. An estimate of the interfacial shear strength using the Kelly-Tyson approach is also shown. The Kelly-Tyson values are considerably lower than the values obtained using the Cox model with the elastic and secant modulus values. This is to be expected since the Kelly-Tyson values represent the average shear stress, while the Cox model refers to peak values.

CONCLUSIONS

Interfacial adhesion studies performed on E-glass fibers in a model polyisocyanurate resin showed that the polyisocyanurate network exhibited pronounced viscoelastic behavior during the test. This behavior was consistent with results obtained on previous work on an epoxy matrix. Although excellent agreement is obtained for the initial strain increments, the actual load in the end of the test is approximately 45 % lower than the value predicted by the linear elastic load time curve. In addition, the first fragment break appears when the actual load in the matrix has deviated from the linear elastic prediction. Previous calculations on DGEBA/m-PDA SFFT specimens have shown that the linear viscoelastic prediction (not shown) does not provide a reasonable estimate of the actual load-time curve. As with the DGEBA/m-PDA SFFT specimens, the relaxation behavior of the matrix, within each step, becomes more pronounced as the strain is increased. This behavior is consistent with nonlinear viscoelastic behavior. Samples were strained at three different rates and, even though the total time of the test ranged from 6 h to 36 h for the different rates, the distributions and number of breaks were similar, thus indicating that the strain rate does not affect the fragment distribution at saturation. This conclusion contrasts with the conclusion obtained in previous work on epoxy specimens.

REFERENCES

1. Kelly, A., and Tyson, W., "Tensile Properties of Fibre-Reinforced Metals: Copper/Tungsten and Copper/Molybdenum, *J. Mech. Phys. Solids* **13**, 329, (1965).
2. McDonough, W., Schutte, C., Moon, C., Schultheisz, C., and Dunkers, J., "Processing and Testing Issues for a Model Polyisocyanurate/Glass Single Fiber Composite," *10ᵗʰ Annual ASM/ESD Advanced Composites Conference*, 535-544, (1994).
3. Drzal, L., and Herrera-Franco, P., "Composite Fiber-Matrix Bond Tests," Engineered Materials Handbook: Adhesive and Sealants, Vol 3 (ASM International, Metals Park, Ohio), 391-405, (1990).
4. Moon, C. and McDonough, W., private communication
5. Holmes, G., Peterson, R., Hunston, D., and McDonough, W., "The Influence of the Matrix Modulus on the Interfacial Shear Strength Parameter," 21ˢᵗ Annual Meeting of the Adhesion Society, 175-178, (1998).
6. McDonough, W., Holmes, G., Hunston, D., and Parnas, R., *Workshop on Micro-Mechanics Measurement Technologies for Fiber-Polymer Interfaces*, National Institute of Standards and Technology Internal Report #6102, (1997).
7. Certain commercial materials and equipment are identified in this paper to specify adequately the experimental procedure. In no case does such identification imply recommendation or endorsement by the National Institute of Standards and Technology, nor does it imply necessarily that the product is the best available for the purpose.
8. Hunston, D., Holmes, G., and Peterson, R., "Viscoelastic Properties of a Resin Commonly Used in the Single Fiber Fragmentation Test," to be published in Proceedings of the Amer. Soc. For Composites, (1998).
9. Holmes, G., Peterson, R., Hunston, D., McDonough, W., and Schutte, C., "The Effect of Nonlinear Viscoelasticity on Interfacial Shear Strength Measurements," to be published in ASTM STP 1357 American Society for Testing and Materials.
10. Schultheisz, C., Schutte, C., McDonough, W., MacTurk, K., McAuliffe, M., Kondagunta, S., and Hunston, D., "Effect of Temperature and Fiber Coating on the Strength of E-

Glass Fibers and the E-Glass/Epoxy Interface for Single-Fiber Fragmentation Samples Immersed in Water," *Fiber, Matrix, and Interface Properties*, ASTM STP 1290, 103-131, (1996).

11.   Whitney, J., and Drzal, L., "Axisymmetric Stress Distribution Around an Isolated Fiber Fragment," Toughened Composites, ASTM STP 937, American Society for Testing and Materials, 179-196, (1987).

TABLE I
Calculations of interfacial shear strength

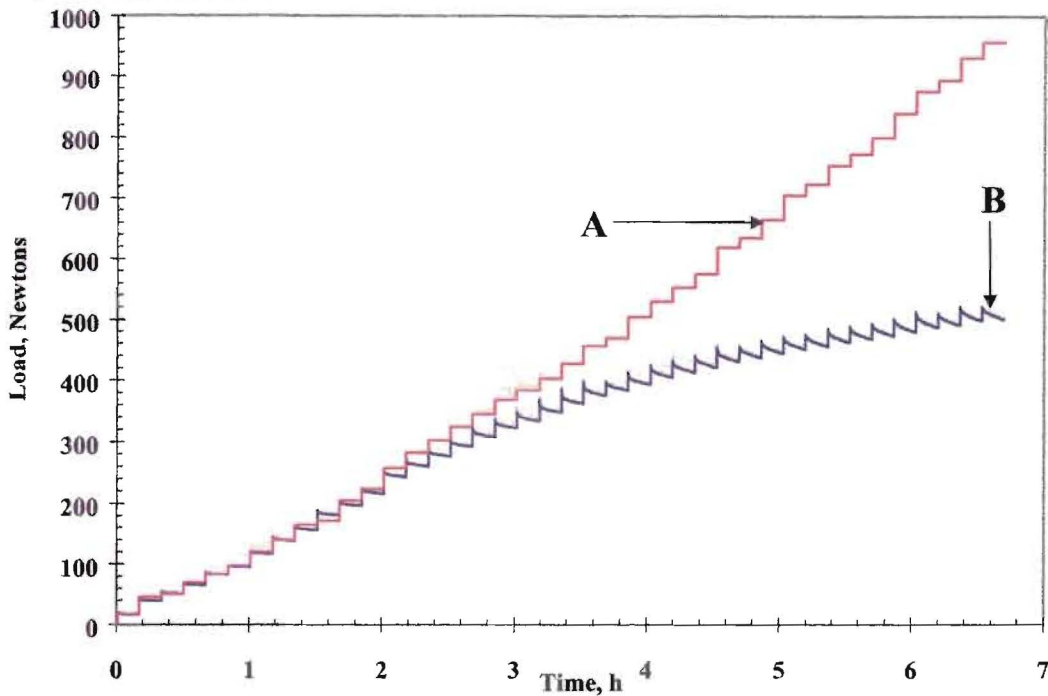| Specimen		Specimen 1	Specimen 2	Specimen 3	Specimen 3
Fiber Modulus, GPa		67.5	67.5	67.5	67.5
Poisson's Ratio for the matrix		0.35	0.35	0.35	0.35
Fiber Strength at the Critical Length, GPa		2.025	2.025	2.025	1.849
Specimen Thickness, mm		2.08	2.28	1.80	1.80
Radius of the Matrix, mm		1.04	1.14	0.90	0.90
Fiber Diameter, mm		0.0156	0.0146	0.0164	0.0164
Critical Fragment Length at Saturation, mm		0.4168	0.4213	0.3959	0.3959
Mean and std dev of fragments, mm		312.6 ± 77.6	316.0 ± 69.6	297.0 ± 68.8	297.0 ± 68.8
Elastic Matrix Modulus, GPa (10)		3.06	3.06	3.06	3.06
	β, mm^{-1}	10.87	10.70	11.09	11.09
	τ, MPa	105.7	97.4	125.8	105.5
Pseudo Elastic Modulus GPa (9)		2.72	2.72	2.72	2.72
	β, mm^{-1}	10.22	10.06	10.43	10.43
	τ, MPa	102.5	94.4	122.1	102.4
Secant Modulus at Saturation, GPa (9)		1.89	1.78	1.79	1.88
	β, mm^{-1}	8.46	8.06	8.40	8.62
	τ, MPa	94.5	86.1	111.8	94.6
Kelly-Tyson, Elastic Perfectly Plastic (1)	τ, MPa	37.9	35.0	45.8	38.4

Figure 1. Load time profile of a polyisocyanurate/glass single fiber fragmentation specimen. Curve A is the expected response for a linear elastic material. Curve B is the actual test data for the specimen step-strained at 10 min time intervals.
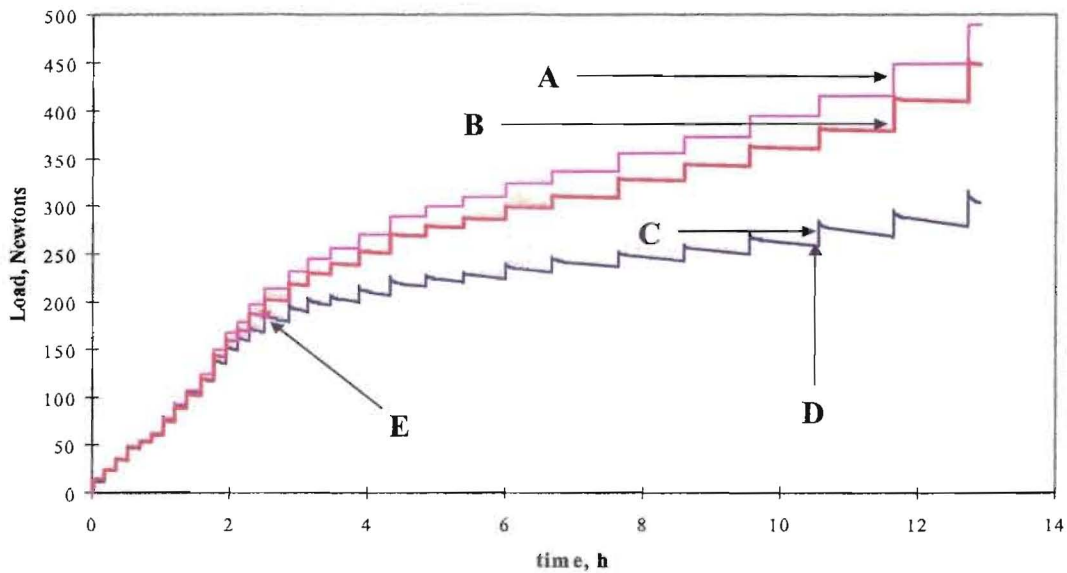

Figure 2. Load vs. time data for a DGEBA/mPDA single fiber fragmentation specimen. Curve A is the theoretical linear elastic load-time curve, curve B is the theoretical linear viscoelastic load time curve, and curve C is the actual load-time curve. D is where saturation occurred, and E is where the first break occurred.
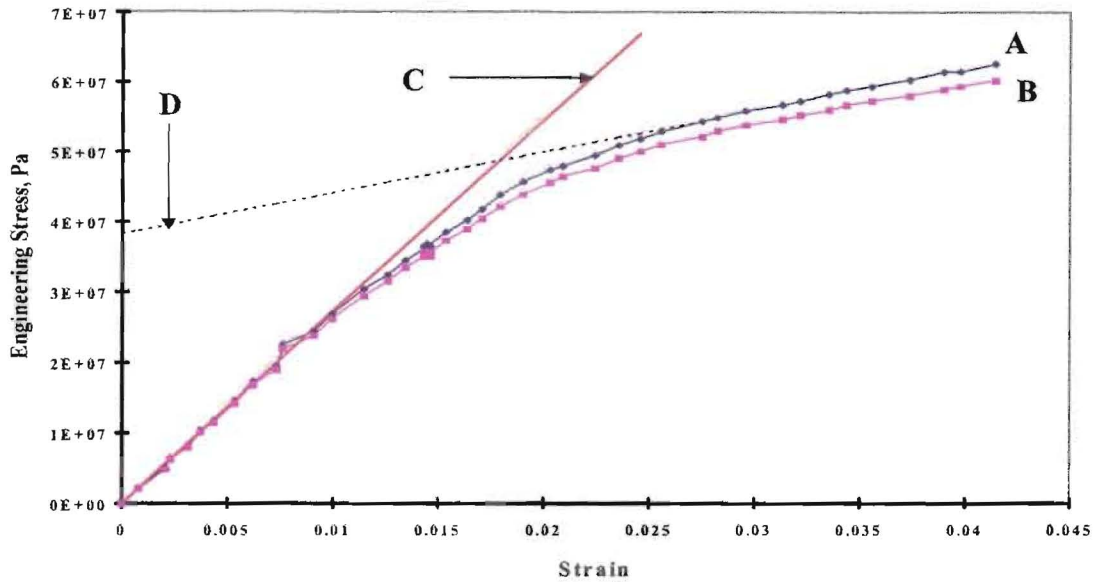
Figure 3. Pseudo-isochronal stress vs. strain plot. From the data shown in Figure 1, curve A represents the stress 10 s after the peak stress at each strain increment and curve B represents the stress at 10 min. Curve C is the regression fit for the 10 s data before the first break and curve D is the regression fit for the 10 s data after the first break.
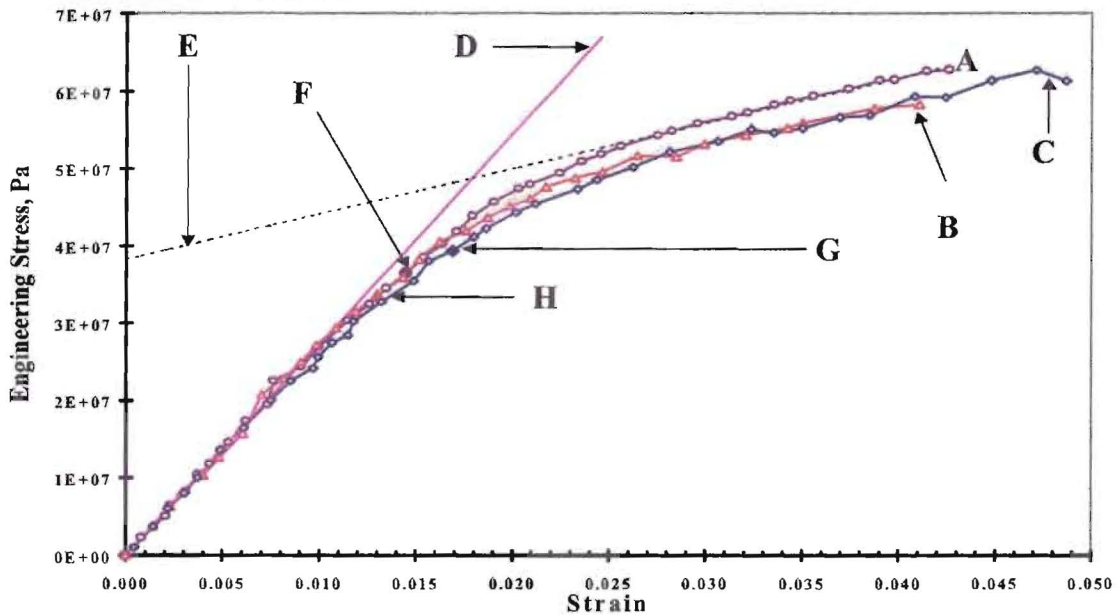

Figure 4. Stress vs. strain 10 s after each strain increment for the three specimens tested. Curve A is data for the 10 min pause with the first break occurring at F. Curve B is for the variable pause with the first break occurring at H. Curve C is data for the 1 h pause with the first break occurring at G. Curve D is for the small strain tangent modulus and Curve E is for the large strain tangent modulus.
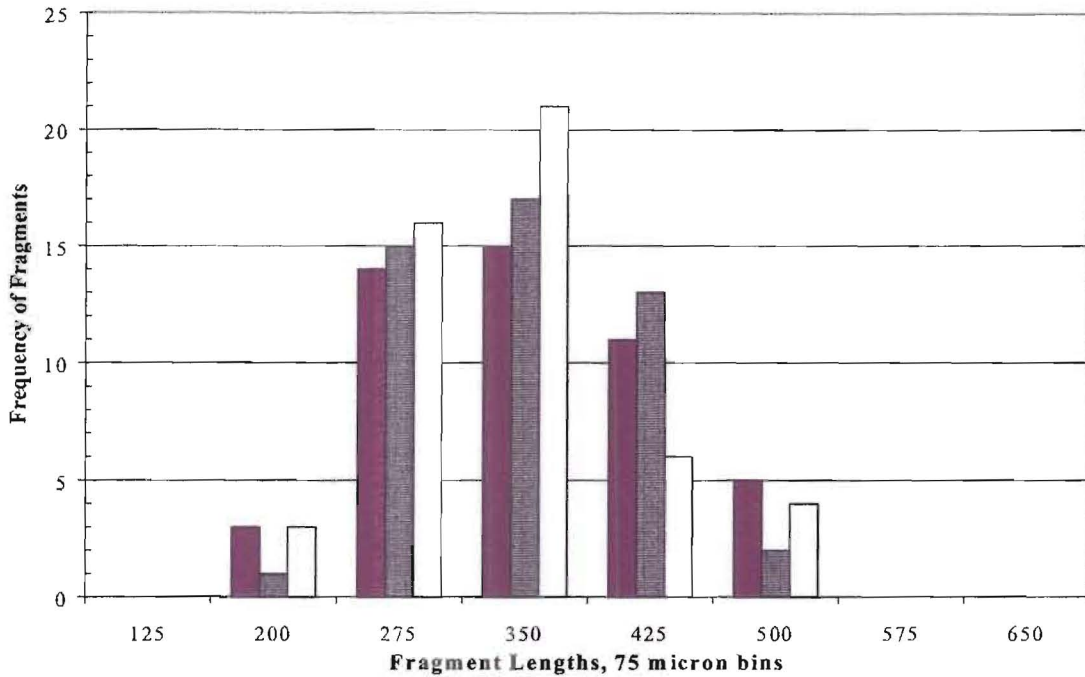
Figure 5. Fragment distribution at saturation for three SFFT specimens. The dark solid bars are for the specimen with 10 min pauses between strain increments, the hatched bars represent the specimen with variable time pauses between strain increments, and the white bars represent the specimen with 1 h pauses between strain increments.
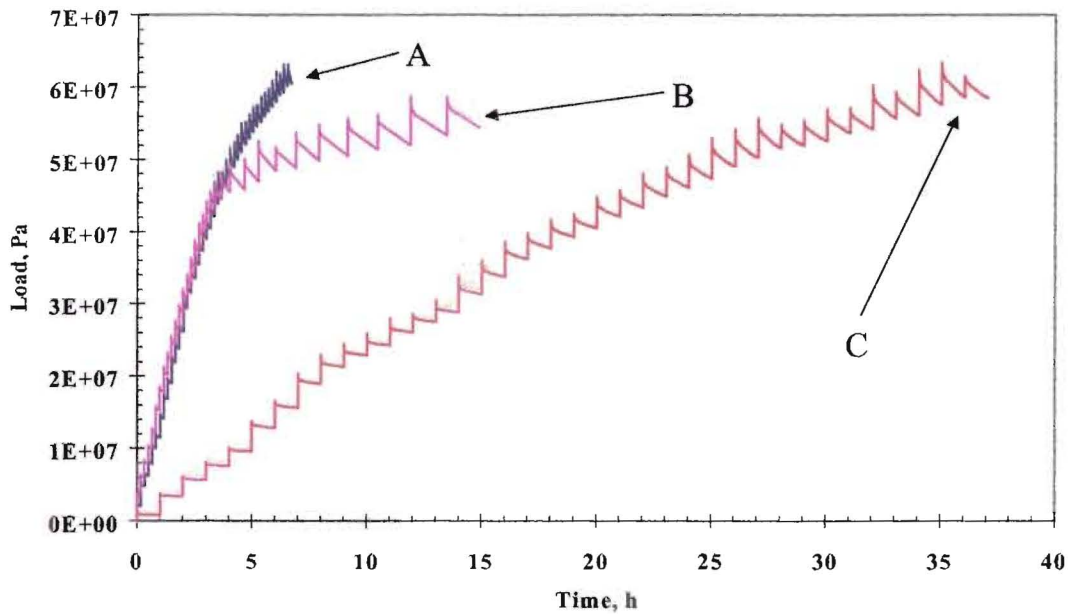

Figure 6. Load vs. time for the three samples tested. Curve A is the data for the 10 min pause, Curve B is the data for the variable time pause, and Curve C is the data for the 1 h pause.
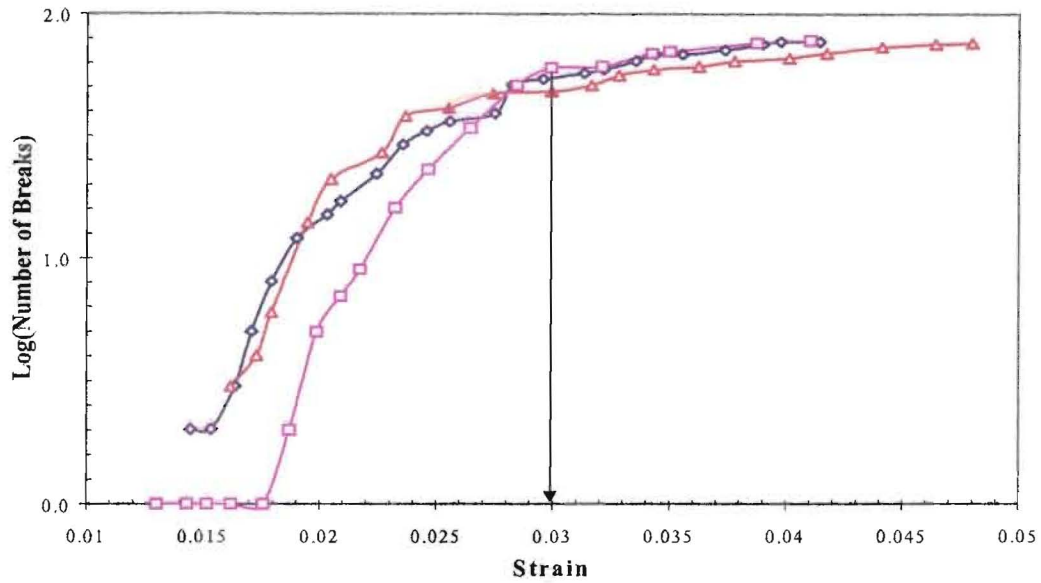
Figure 7. Log (number of breaks in the fiber) vs. strain for the three specimens tested. The curve with diamonds represents the 10 min pause data, the curve with the squares represents the variable time data, and the curve with the triangles represents the 1 h pause data.